JOURNAL OF PROPULSION AND POWER
Vol. 26, No. 4, July–August 2010

Combustion of Silicon/Teflon/Viton and Aluminum/Teflon/Viton Energetic Composites

Cole D. Yarrington* and Steven F. Son†
Purdue University, West Lafayette, Indiana 47906
and
Timothy J. Foley‡
Los Alamos National Laboratory, Los Alamos, New Mexico 87544

DOI: 10.2514/1.46182

The combustion of Si- and Al-based systems using polytetrafluoroethylene (PTFE) as the oxidizer and Fluorel FC 2175 (a copolymer of hexafluoropropylene and vinylidene fluoride) as a binder has been studied. Experimental data were obtained using two methods: 1) instrumented tube burns and 2) pressed pellets inside a windowed pressure vessel. Loose-powder burning rates were seen to optimize at slightly-fuel-rich mixture ratios for Si/PTFE/FC-2175 (SiTV). Al/PTFE/FC-2175 (AlTV) burning rates optimized near a stoichiometric ratio. Pressures calculated by assuming constant-volume combustion equilibrium were seen to match experimental values from burn-tube experiments when burning rates were at or near peak values. The pressure dependence of SiTV and AlTV pellet burning rates was also characterized and compared with reported Mg/PTFE/Viton (MTV) results. SiTV showed power-law dependence with a constant-pressure exponent over the experimental range of pressures. AlTV was shown to exhibit nonconstant-pressure exponent behavior. SiTV burning rates optimized at mixture ratios similar to that of the tube burns. AlTV burning rates increased well past a stoichiometric ratio and decreased at a fuel-rich ratio, which is a similar trend to MTV burning rates.

I. Introduction

SILICON has been used as an ingredient in pyrotechnic compositions for delays and ignition [1]; however, the combustion of nanoscale Si powders has not been extensively studied. Applications such as destroying chemical or biological agents (technologies such as these are generally termed *agent defeat*) may also be of interest for these systems because of the hot corrosive properties of SiF_x products and the production of HF. In the following we will briefly review some of the relevant literature.

The combustion of microscale Si reactives has been reported in the literature. Burning rates were found for various mixture ratios of 2–5 μm Si with PbO by Al-Kazraji and Rees [2], who reported burning rates for pressed pellets as high as 26 cm/s. Al-Kazraji and Rees also reported that the burning rate decreased with larger Si particle sizes, and the range for sustainable combustion was 20–50 wt % Si. Rugunanan and Brown [3] investigated the combustion of Si with Fe_2O_3 and SnO_2. He also reports sustainable combustion ranges of 20–40 and 20–55 wt% Si for Fe_2O_3 and SnO_2 respectively. The particles used by Rugunanan and Brown were all nominally greater than 3 μm and many had broad distributions of particles sizes. Burning rates for pressed pellets of Si with Fe_2O_3 and SnO_2 ranged from 2.3–5.7 mm/s and 5.3–17.0 mm/s respectively. Rugunanan and Brown also studied the combustion of these same Si particles with Sb_2O_3 and KNO_3 [4]. They report burning rates of 1.6–8.5 mm/s for Sb_2O_3, and 1.7–34.5 mm/s for KNO_3. The maximum temperatures measured using embedded thermocouples for all of these mixtures ranged from 1230 to around 1700°C. These temperatures are far below predicted values. The effect of ambient pressure was not studied.

Explosive properties of nanostructured Si were first recognized in 1992 [5] in an experiment designed to investigate the source of chemiluminescence of porous Si. Fan et al. [6] also hinted at a violent reaction of the Si/PbO system under mechanical alloying conditions in a ball mill, although the occurrence of an explosion is only inferred. In 2001, a violent reaction of Si with cryogenic oxygen was observed by Kovalev et al. [7]. In this experiment, hydrogen-terminated porous Si was filled with liquid oxygen, resulting in an vigorous reaction.

The recent discovery and renewed interest in Si as a highly reactive material can be attributed to the dependence of reactivity on particle or pore size. This dependence has been shown for Al, where microscale particles ($\geq$ 100 nm) are much less reactive than nanoparticles [8]. One conclusion that is drawn from the work of Fan et al. [6] is that in a ball mill, the Si/PbO reaction does not take place until the particles are nanoscale. Because of this scale dependence, much of the recent Si reactives work has been done using nanoporous Si as the reactive as it can be manufactured using readily available technology from the semiconductor industry. Mikulec et al. [9] were the first to form a composite solid-state reactive composite on a Si wafer. Clément et al. [10] performed a detailed study of Si etching and related morphology, solid oxidizer loading, and the related reactive properties. A thorough review of past Si energetics research was prepared by Koch and Clément [1].

As Si nanopowders become more readily available it is worthwhile to revisit the combustion properties of Si-based systems, as they are likely to be different from past work based on microscale Si particles ($\geq$ 100 nm). It is also much easier to vary the stoichiometric ratios when working with powders compared with etched porous Si wafers, where stoichiometries are determined by pore sizes, pore structures, surface properties of fuel and oxidizer, and pore filling methods. To the authors' knowledge, combustion of Si reactives with fluorine-based oxidizers has not been reported in the literature. However, thermal analysis [11] and combustion synthesis of novel carbon and inorganic 1-D nanostructures [12] using Si and polytetrafluoroethylene (PTFE) have been reported.

The dependence of combustion properties on particle size has been well documented for Al-based nanoenergetics using oxygen-based

Presented as Paper 2009-760 at the Aerospace Sciences Meeting, Orlando, FL, 5–8 January 2009; received 30 June 2009; revision received 22 February 2010; accepted for publication 23 February 2010.

*Research Assistant, Mechanical Engineering; cyarring@purdue.edu. Member AIAA.
†Associate Professor, Mechanical Engineering; sson@purdue.edu. Member AIAA.
‡Project Manager; tfoley@lanl.gov.

oxidizers [8,13]. Some Al work has also been done using fluorinated oxidizers. Osborne and Pantoya [14] outlined a low-temperature preignition reaction caused by the fluorination of the oxide layer present on the Al particles. Zamkov et al. [15] analyzed the combustion of Al with PTFE using time-resolved infrared spectroscopy. Dolgoborodov et al. [16] also recorded very high speeds in Al/PTFE reactive powder systems, ranging from 700 to 1300 m/s. More recently, Watson et al. [17] investigated the combustion of nano Al with PTFE and MoO_3. They found that the high volume of gas produced in Al/PTFE powders results in higher speeds when the combustion is confined. They note that the higher pressures seen in confined burns does not directly correlate to faster speeds as a general rule, as the lower-pressure Al/MoO_3 still showed higher speeds. No studies have considered the effect of pressure on the combustion.

Insight can also be gained by comparing similar combustion systems. Magnesium is used in Mg/PTFE/Viton (MTV), and this system has been widely studied. MTV is a common pyrolant used in a variety of applications, such decoy flares, tracking flares, countermeasure torches, tracer units, igniters, etc. [18]. Kubota and Serizawa [19] studied the effects of stoichiometry, Mg particle size, and adiabatic flame temperature and pressure on the burning rate of Mg and PTFE. They found that although the calculated temperature optimizes at a Mg weight fraction of 0.33, the burning rate increases with Mg weight fraction beyond this. They concluded that the burning rate does not depend on the final flame temperature. The burning rate increased continuously up to mixture ratios as large as 70/30 Mg/PTFE (3 wt% Viton added), at which point no more data were reported. They also found that smaller Mg particle size resulted in faster burning rates. The smallest-size Mg particle considered was 22 μm. Kuwahara et al. [20] looked closely at the effect of Mg weight fraction and pressure on the burning rate, finding that increasing Mg weight fraction leads to a drastically different pressure dependence. Fitting their burning-rate-vs-pressure curves with a typical power-law curve, they found pressure exponents that differed by an order of magnitude over the range of weight fractions investigated. Koch [21] also performed a detailed investigation on the combustion of MTV. In that paper, he presents data from differential scanning calorimetry (DSC), differential thermal analysis, and differential thermal gravimetry. Based on his experimental results Koch proposes a combustion mechanism that includes two primary reactions and five aerobic or afterburn reactions. Koch also proposed a burning-rate model for the MTV system.

Note that Teflon® and Viton® are registered trademarks of DuPont and have been used here to abbreviate certain composites [Si/PTFE/FC-2175 (SiTV), Al/PTFE/FC-2175 (AlTV), and MTV], consistent with the literature. However, the specific materials used in these composites are not Teflon and Viton, but chemically equivalent products. The specific materials used, not the registered trademarks, will be referenced throughout this paper, except in the use of the abbreviated composite names SiTV, AlTV, and MTV.

This study will examine the fundamental combustion properties of SiTV and AlTV systems, such as burning rate as a function of pressure. The burning rate as a function of stoichiometry will also be presented for pressed pellets and loose powders. We will present thermochemical calculations of temperature and product species.

II. Equilibrium Calculations

The general stoichiometric equations for the reaction of Si or Al with PTFE,

$$\mathrm{Si} + \mathrm{C_2F_4} \longrightarrow 2\mathrm{C} + \mathrm{SiF_4} \tag{1}$$

$$4\mathrm{Al} + 3\mathrm{C_2F_4} \longrightarrow 6\mathrm{C} + 4\mathrm{AlF_3} \tag{2}$$

are useful for the calculation of properties such as equivalence ratio and heat of reaction, but they do not reflect the true nature of the combustion event. For more detailed predictions, equilibrium codes can be used. The chemical equilibrium software Cheetah 4.0 that was developed at Lawrence Livermore National Laboratories by Fried et al. [22] was used to predict temperatures, gas volumes, and product concentrations of the composites studied as part of this work. The Cheetah equilibrium results were also used as a tool in choosing the initial mixture ratios of the composites. Shown in Figs. 1 and 2 are results from the equilibrium calculations for SiTV and AlTV using 10% FC-2175 at constant atmospheric pressure. It is also important to note that the experimentally measured amount of metal oxide was also included in these calculations. The active fuel content of Al and Si are listed in Table 1. Table 2 lists melting and vaporization/decomposition temperatures of the significant reactants and products. A significant result from the predictions is that when using PTFE as an oxidizer, the calculated equilibrium temperature of the Si system is higher than that of the Al system ($T_{\max,\mathrm{Si}} = 3471$ K and $T_{\max,\mathrm{Al}} = 3391$ K). This is not the case with oxygen-based systems, in which Al-based composites have a higher reaction temperature. This is likely due to the difference in natural oxidation layer on the different metals. When the metal passivation layers are not included in the calculations, the temperatures are essentially equal at 3508 K.

Cheetah 4.0 calculations were also done for these composites without the presence of FC-2175. The results of these calculations did not significantly differ qualitatively from the results presented here, although there are slight quantitative differences. The calculated equilibrium temperatures for Si/PTFE and Al/PTFE are 58 and 53 K higher than SiTV and AlTV with 10 wt% FC-2175. Also, because the Si/PTFE and Al/PTFE systems have no hydrogen addition from the binder, the calculated gas volume is 208 and 93 $\mathrm{cm^3/g}$ lower, respectively, than for SiTV and AlTV with 10 wt% FC-2175.

The specific volume of gas products is slightly higher for Al than for Si. The mixture ratio at which the maximum temperature occurs is at a slightly higher equivalence ratio for the Si-based systems ($\phi_{\mathrm{Si}} = 1.29$ and $\phi_{\mathrm{Al}} = 1.26$). Also of note is the relatively flat temperature profile of the Si system from 33–51 wt% Si, which may be a result of the Si carbide in the system, which has a melting point

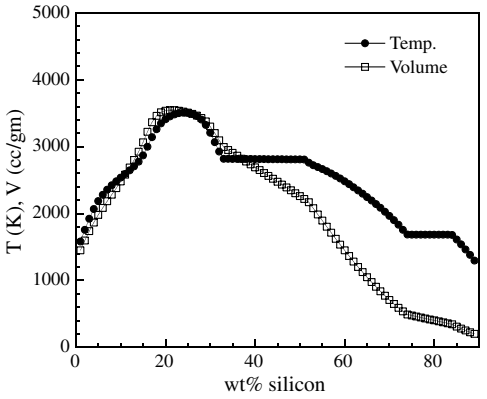

a) Temperature and gas volume

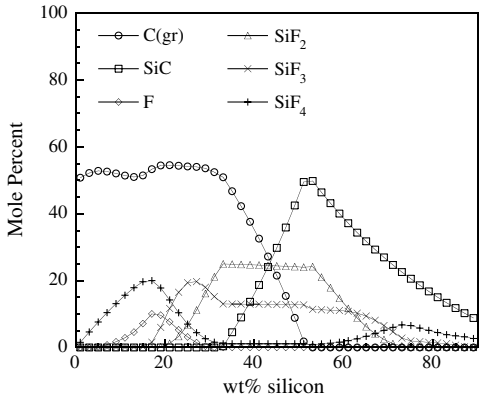

b) Product mole percentages

Fig. 1 Cheetah 4.0 equilibrium calculation results for Si/PTFE and 10% FC-2175 at constant atmospheric pressure.

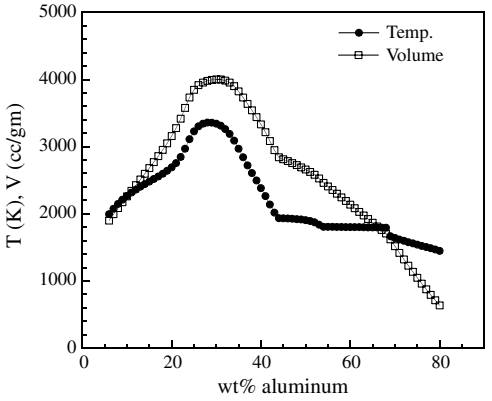

a) Temperature and gas volume

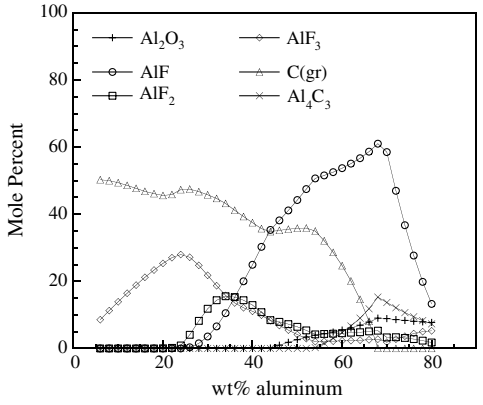

b) Product mole percentages

Fig. 2 Cheetah 4.0 equilibrium calculation results for Al/PTFE and 10% FC-2175 at constant atmospheric pressure.

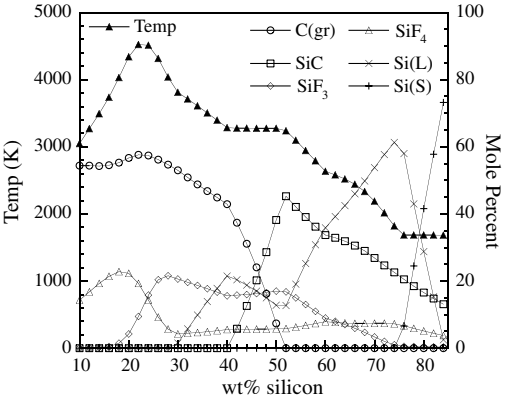

a) SiTV temperature and products

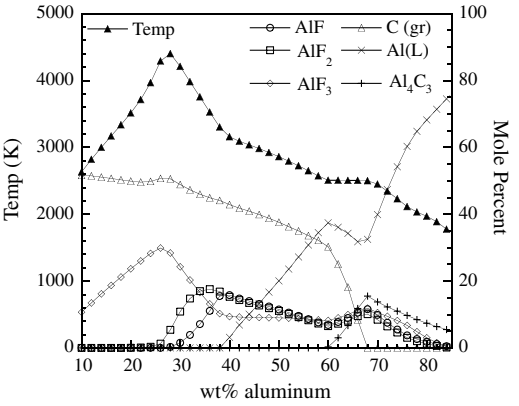

b) AlTV temperature and products

Fig. 3 Cheetah 4.0 constant-volume equilibrium calculation results for AlTV and SiTV with 10% FC-2175.

around 2700°C. The Al calculations show a similar plateau from 50–63 wt% Al that is attributed to Al carbide (similar to the Si system) and is stable up to 1400°C. Both systems are predicted to oxidize with multiple oxidation states: e.g., SiF_4, SiF_3, and SiF_2. These products shift to lower molecular weight molecules (e.g., SiF_2 compared with SiF_4) as the mixture ratio becomes more fuel-rich and less fluorine is available. The exception to this trend can be seen at very fuel-rich stoichiometries (wt% Al > 75, wt% Si > 70), in which the temperature is not very high and the concentrations of the more stable SiF_4 and AlF_3 molecules peak and the others decline.

Constant-volume equilibrium calculations were also performed and the results are shown in Fig. 3. The results of these calculations differed slightly from the constant-pressure equilibrium results reported above. The main difference is that the maximum equilibrium temperature is much higher with a constant volume ($T_{max,Si} = 4546$ K and $T_{max,Al} = 4404$ K). The equilibrium products differed only in the presence of liquid Si in the constant-volume calculation, which is absent in the constant-pressure results. This result is easily explained by the much higher pressures predicted with the constant-volume assumption.

A straightforward application of Glassman's [26] criterion for the vapor-phase combustion of metals is not possible for the case of fluorinated oxidizers, because the flame temperature is not a specific known value as it is for metals burning in oxygen. However, the adiabatic flame temperatures can be compared with the metal vaporization temperature to predict whether the combustion occurs homogeneously or heterogeneously. Figure 4a shows that SiTV is expected to burn heterogeneously at all pressures and mixture ratios. From Fig. 4b it is seen that AlTV is expected to burn heterogeneously at certain mixture ratios, but at temperatures near the maximum

Table 1 Shown here are the material descriptions, physical properties, and suppliers

Description	% active content	Size	SSA,[a] m^2/gm	Supplier
Amorphous nano Si powder	93[b]	50 nm	≥ 80[c]	Sigma Aldrich, Inc.
Nano Al powder	79	80 nm	28[c]	Novacentrix Corp.
Fluorel FC 2175 binder	100	solution	N/A	Mach I, Inc.
Zonyl MP1100 PTFE powder	100	200 nm	5–10[c]	DuPont

[a]SSA denotes specific surface area. [b]Measured by a volumetric method [23]. [c]As reported by supplier.

Table 2 Melting and vaporization temperatures for major reactants and products of AlTV and SiTV

Property[a]	Si	SiO_2	SiF_4	SiC	Al	Al_2O_3	AlF_3	Al_4C_3	PTFE[b]
T_{melt}, K	1687	1986	183	3103	933	2327	1549	2373	600
T_{vap} or T_{decomp}, K	3538	3223	187	N/A	2792	3250	1549	>2473	N/A

[a]Unless otherwise specified, properties come from [24]. [b]Material selector [25].

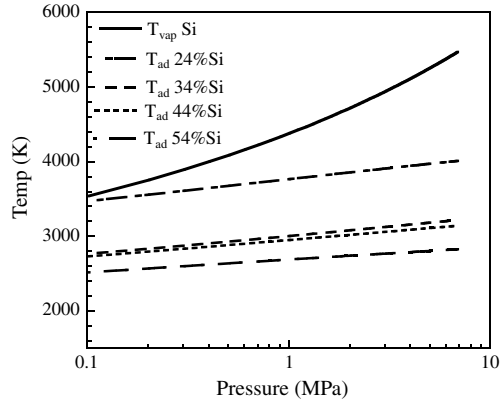

a) SiTV T_{vap} and T_{adab}

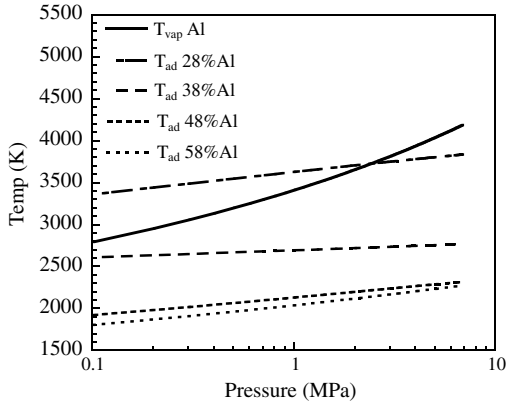

b) AlTV T_{vap} and T_{adab}

Fig. 4 Plots of Si and Al T_{vap} along with SiTV and AlTV T_{adab} for different mixture ratios plotted vs pressure.

expected temperatures, it may burn either homogeneously or heterogeneously, depending on the pressure.

III. Experimental

A. Materials and Sample Preparation

The materials used and their physical properties can be found in Table 2. Both the Al and Si nanomaterials develop a passivation layer during the manufacturing process. The passivation layer of the Al used in this study (typically 2 nm) is manufactured carefully to a tight tolerance and is smaller than a typical Al passivation layer (4–6 nm) that is found on industrial Al. Much care is taken to prevent the nanoscale Al from being exposed to oxygen and growing the passivation layer. The nanoscale Si passivation is not subject to such measures and is typically around 1–2 nm thick naturally. This is advantageous for Si, because the smaller passivation layer for a given size translates to higher active fuel content. Both the Al and the Si as received are held in a low-oxygen and low-moisture argon environment to inhibit growth of the oxide layers. Fluorel FC 2175 is sold under a different name but is chemically equivalent to Viton.

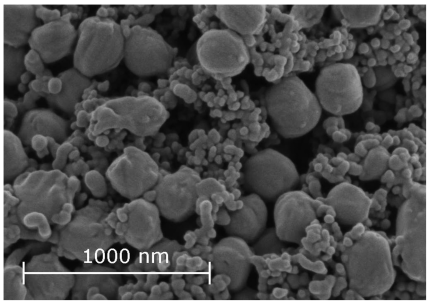

Fig. 5 SEM image of SiTV with 5 wt% FC-2175.

A shock-gel process was used to prepare all powder samples. Scanning electron microscopy (SEM) images of the resultant powder for SiTV with 5 wt% FC-2175 are shown in Fig. 5. In this image, the larger spherical particles are PTFE and the smaller particles are Si. The FC-2175 is coated on the particle surfaces and so cannot be distinguished. The shock-gel process is described in detail in military specifications [27] for MTV. In the shock-gel process, the desired amount of FC 2175 is dissolved in acetone. PTFE is then added to the mixture, which is then sonicated (using a Branson Digital Sonicator 450 with tip type 102C) to break up agglomerates. The sonicator was set to an output power of 200 W with a duty cycle of 80% and a period of 1 s. Silicon (or Al) is then added to the mixture in the specified amount. The mixture may not have the desired consistency, so more acetone can be added. The mixture is again sonicated, after which a sufficient amount of hexane is rapidly added to precipitate out all of the FC 2175. Hexane addition is done while keeping the mixture sufficiently suspended and mixed so the FC 2175 coats the particles evenly and uniformly. The mixture is then poured into a stainless steel pan and placed inside a vented hood and on a hot plate to dry. After the mixture is completely dry it is run through a sieve and placed in conductive vials. To ensure complete drying of the composites, the vials are also placed in a rough vacuum oven at 14.4 kPa (107 Torr) and 70°C.

Initial component weight percentages were chosen based on the maximum temperature stoichiometries (24% Si and 28% Al) predicted by equilibrium calculations. Additional mixture ratios were also prepared. Table 3 shows the percentage of each component used for all experiments.

B. Loose-Powder Tube Burns

Loose-powder instrumented tube burns were performed using either a polycarbonate or a stainless steel structural block, into which is inserted a 0.375-cm-i.d. acrylic tube. Six optical fibers are spaced 1 cm apart and coupled to photodiodes (ThorLabs model DET 10A) to detect light emission from the combustion. Six pressure transducers (PCB Piezotronics model 113A22) are also spaced 1 cm apart on the opposite side and measure the instantaneous pressure at those points. A Nonel shock tube is held in place at the end of the tube by a compression fitting that attaches to the structural block. The tube is inserted a measured distance such that it is inside of the acrylic tube and in direct contact with the energetic composite. The whole ignition setup is secured such that a fixed wall boundary condition is approximated. Some earlier experiments presented here were performed without a closed-end configuration by placing the shock tube in the acrylic tube and securing it with tape. A Nonel shock tube is hollow plastic tubing, with the inner wall coated with fine powdered explosive. A shock wave propagates down the tube and ignites the energetic material inside the acrylic tube. A similar burn tube (without Nonel) was first used and described by Bockmon et al. [13] The data were recorded using three Tektronix TDS 2004B oscilloscopes. The complete instrumented tube-burn setup is secured inside a fragmentation box and ignited. The first photodiode was used as the data trigger.

Several initiation techniques were tested, and Nonel shock tube ignition provided the best consistency for Si-based composites. Although the Si-based reactives were more difficult to ignite, they tend to be less sensitive in general to various stimuli. SiTV at 24 wt% Si and 10 wt% FC-2175 were tested for spark sensitivity and did not react at the instrument limit, which is 1300 mJ. Hammer tests also indicated that SiTV is not very sensitive to mechanical stimulus.

Table 3 Shown here are the component weight percentages used in all experiments

Composite	% FC-2175	% PTFE	% Si	% Al
SiTV	10 or 15	76/66/56/46/36	14/24/34/44/54	0
AlTV	10	62/52/42/32	0	28/38/48/58

When initiation frequently failed for Si fuels, the Al fueled composites successfully ignited using methods other than Nonel. Ignition with nichrome (NiCr) wire for Al, as well as Nonel ignition for both Al and Si are presented later in this paper. Each tube was loaded with the Si or Al composite and the mass measured for calculation of the powder density. The densities of all tube burns were between 13 and 17% theoretical maximum density (TMD). The difference in densities results mainly from the varying equivalence ratios and the different packing properties of the base reactants.

C. Pressed Pellets and Crawford Bomb

Powders were weighed and then poured into a 0.635 cm pellet pressing die. Using a remote press, the samples experienced a pressure of 352 MPa for 10 min. Using this pressure, samples were pressed to TMDs that varied depending on mixture ratio (95–99% TMD for AlTV and 78–98% TMD for SiTV) and to a length of around 0.5 cm. Initial studies of pressed pellets of Si and PTFE without binder resulted in pellets that were brittle to the touch and would break during handling or if dropped from a short height ($\sim$10–20 cm). These same pellets would burn normally under atmospheric pressure, but would explode when burned at pressures above atmospheric. It is believed that the binderless pellets formed laminate layers during processing, which resulted in a porous pellet rather than a pellet with uniformly distributed particles and no voids. During combustion under pressure, this would result in flame propagation down voids and a resultant overpressure that would destroy the sample. The addition of a small amount of binder (FC-2175) has proven to be a solution to this problem.

The amount of binder was chosen such that the smallest amount of binder necessary to maintain mechanical stability over the range of experiments conducted was used. For pressed pellets of Si-based composites, 15% wt of FC 2175 resulted in mechanically sound pellets for all stoichiometries and pressures that were investigated. The addition of an extra 5% wt FC 2175 from 10% resulted in a decrease of only 30°C in the predicted equilibrium temperature and an increase of 100 cm^3/g in the specific volume of combustion gases. The extra FC 2175 also resulted in a 1% increase in the predicted wt% Si at maximum equilibrium temperature.

After pressing, the pellets were secured to a sample holder with quick-dry epoxy, and a clear paint inhibitor was coated on the outer surface of the pellets to ensure a one-dimensional burn. The pressed pellets were placed in a pressure vessel and ignited by heating NiCr wire that was in contact with the sample. The pressure system was rated to 41 MPa and the pressure vessel had two optical access ports. The samples were ignited and burned in an argon environment. High-speed images were recorded with a Vision Research Phantom model V7.3 camera and were used to determine the propagation speed of the flame front and its dependence on pressure using the video record.

IV. Results

A. Loose-Powder Tube Burns

At least three loose-powder tube burns were conducted for each of the mixture ratios listed in Table 3. Figure 6 shows pressure traces for instrumented tube burns of AlTV using Nonel and NiCr ignition in the original shock tube setup without compression fittings. In both AlTV cases, the data were slightly clipped by the data acquisition system, due to the unexpected magnitude of the peak pressures, which are much higher than thermites [13]. Pressure data were not recorded in subsequent runs, due to the high pressures involved. Also note that the horizontal-axis scale in Fig. 7a is three times larger than in Figs. 6a and 6b, due to the slower burning rate of the SiTV composites. When Nonel is used, the pressure reaches a steady state quickly. By the second transducer, the peak pressure essentially remains constant for the remainder of the burn. The slopes of the traces are also very similar for all of the transducers. In contrast, when NiCr ignition is used, the pressure builds very slowly. At the second transducer, the pressure is still not at a peak, nor has the slope of the pressure trace reached a constant value. Only by the third transducer has the pressure nearly reached a steady state. This is expected

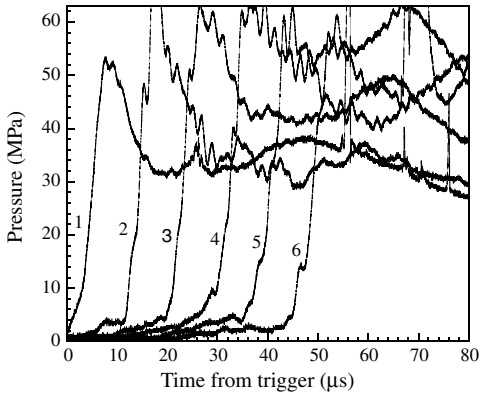

a) AlTV ignited with Nonel ® - pressure vs. time

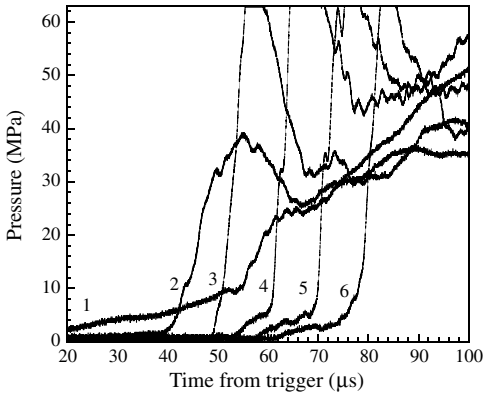

b) AlTV ignited with NiCr wire - pressure vs. time

Fig. 6 Pressure profiles obtained in burn tube with AlTV for different igniters.

qualitatively, as Nonel ignition involves a sharp rise in pressure and high velocity combustion products, and NiCr wire ignition involves only heating at atmospheric pressure. The difference between these two plots is significant, as it leads to different results in the initial propagation rate.

Figure 7a shows pressure traces for SiTV using 10 wt% FC-2175. There are several differences between the pressure traces of SiTV and AlTV. Because of the high gas volume produced in AlTV mixtures, peak pressures often go above 69 MPa. The highest pressure seen for SiTV was 53 MPa, which occurs at 34 wt% Si. Because the SiTV is ignited using Nonel, there is a sharp rise at the first transducer, although the peak pressure continues to rise at each transducer. The burning rate is also not completely steady; however, the largest increase in burning rate occurs from the first to the second transducer. If the reaction propagates fast enough, the burn-tube experiment can be considered as constant-volume [28]. It follows then that the pressure will increase in the tube as material is consumed and gaseous products are produced. The pressure gradient of the SiTV pressure trace is lower than AlTV (2.2 compared with 7.8 MPa/μs for transducer 6), which is expected, due to the slower burning rate and lower gas production of SiTV.

Figure 7b represents three separate burn-tube experiments and highlights the importance of the ignition method used. The only viable method found to ignite SiTV was Nonel. However, AlTV could be ignited in a couple of ways that yielded different results. When AlTV was ignited using Nonel, the speed recorded was constant at around 1070 m/s. When the material was ignited by heating a NiCr wire in contact with material, the burn progressed slowly relative to Nonel ignition ($\sim$200 m/s) at an early time, after which the speed transitioned to the faster rate, at around 1020 m/s. These data indicate a difference in the time to steady state. There is also a very abrupt transition to steady state from the slower burning rate. It is not yet known what conditions affect this acceleration, but a dependence on pressure is likely. In contrast to NiCr ignition, Nonel

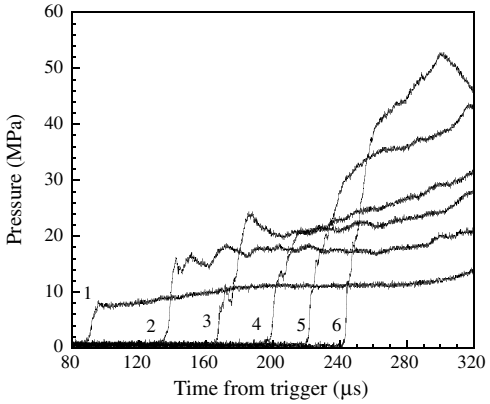

a) SiTV pressure profiles

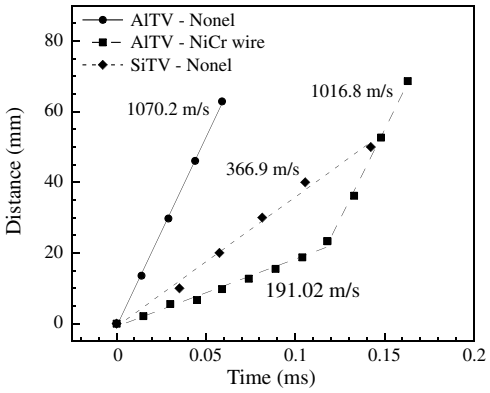

b) SiTV and AlTV burning rates

Fig. 7 SiTV pressure profiles and burning rates for AlTV and SiTV with 10 wt% FC-2175 for different ignition methods.

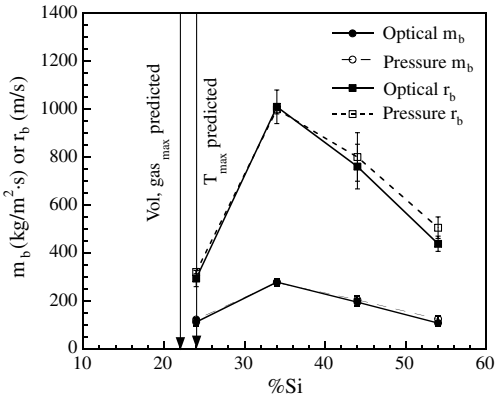

a) SiTV burning rates at different stoichiometries

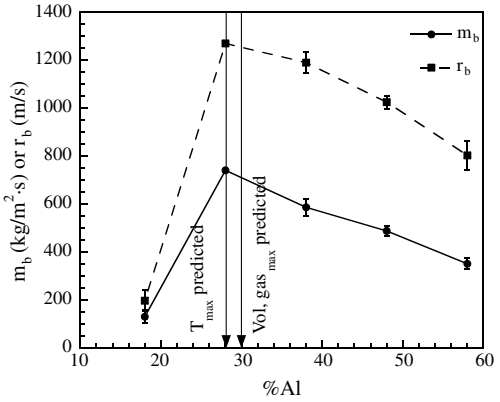

b) AlTV burning rates and mass burning rates at different stoichiometries

Fig. 8 Burning rates and mass burning rates of loose powders of AlTV and SiTV with 10 wt% FC-2175 (m_b is the mass burning rate and r_b is the burning rate).

introduces a pressure pulse as well as hot products. It is possible that pressure must reach a certain level within the burn tube until a higher burning-rate mode can be sustained. The pressure data discussed in the previous paragraph support this hypothesis as well. The presence of an accelerating wave is qualitatively similar to deflagration-to-detonation transition in propellants and explosives.

Shown in Fig. 8 are plots of the average mass burning rates and burning rates taken from both pressure and optical transducers for all of the loose-powder tube burns of SiTV and AlTV with 10 wt% FC-2175. These burns were performed in the closed-end tube-burn configuration. Pressure data were not taken for AlTV because of the high pressures seen, which were much higher than the transducer limit (103 MPa). Measured burning rates are very sensitive to packing density, which is why the mass burning rate is reported here as well as burning rate. The recorded peak pressures and other tube-burn data for SiTV and AlTV are shown in Table 4.

Figure 8a shows the mass burning rates and burning rates of SiTV and AlTV as a function of mixture ratio. Error bars are not visible at some points, because the estimated error at those points is smaller than the symbol size. Figure 8a shows that the maximum predicted temperature mixture ratio for SiTV (24 wt% Si) does not correlate with the maximum burning-rate mixture ratio, which occurs between 24 and 44 wt% Si. AlTV does not show this trend, with the maximum burning rates seen occurring at the maximum predicted temperature mixture ratio (28 wt% Al). Further resolution of the data is needed for both SiTV and AlTV to determine the precise speed-optimized mixture ratio. The maximum (average) burning rate observed was 1010 m/s for SiTV at 34 wt% Si and 1269 m/s for AlTV at 28 wt% Al. Although the exact mixture ratio at which the burning rate is optimized is not known, it is clear that it will occur at fuel-rich conditions for SiTV. This result is not without precedent, as many have observed this before in other systems. Sanders et al. [29] addressed this issue for nanoscale Al thermites and attributed the result for Al/MoO_3 to the presence of liquid products being propelled forward by hot gases, which then solidified upstream of the reaction onto unreacted materials. This convective mode of heat transfer would significantly increase the temperature of the unreacted materials and lead to faster burning rates. Sanders et al. also hypothesized that the presence of hydrated oxidizers or H_2O on the particle surface could result in faster burning rates above stoichiometric ratios, but their model did not indicate sufficient causation to support the data.

The prediction of optimum mixture ratios for burning rate or high pressures in burn tubes would be a useful capability in evaluating and testing energetic materials of this type. As mentioned before, the combustion in the burn-tube experiment may be assumed to occur in a constant-volume if the propagation rate is fast enough. As long as the reaction proceeds at a rate that greatly exceeds the rate of pressure dissipation, the constant-volume assumption should be reasonable. At slower rates the pressure will simply bleed off and a constant-volume assumption is not valid. Shown in Fig. 9 are pressures recorded from burn-tube experiments of SiTV compared with predicted pressures from Cheetah and NASA Chemical Equilibrium with Applications (CEA) [30] equilibrium codes. Calculations were done with both codes in order to have more than one comparison with theoretical. Comparing this plot with Fig. 8a, one sees that the predicted pressures agree well with the experimental values at mixture ratios for which propagation rates are the fastest. This validates the constant-volume assumption at these points; however, the utility of these calculations as a predictive tool is lessened by the fact that the constant-volume assumption is not valid at all points. This is most obviously seen at the first point (24 wt% Si), for which slow propagation rates allow the pressure to dissipate, and the predicted pressure is much different from the actual condition. The calculations do still serve as a useful first step in evaluating and understanding the combustion of these materials.

Table 4 Shown here are the data for instrumented tube burns of SiTV and AlTV; fuel amounts are in wt%

Property	14% Si	24% Si	34% Si	44% Si	54% Si
	SiTV				
Optical burning rate (avg), m/s	N/A	294	1010	761	439
Optical mass burning rate (avg), m/s	N/A	112	279	195	108
Peak P, MPa	N/A	31.7	104.8	71.7	33.1
	AlTV				
Property	18% Al	28% Al	38% Al	48% Al	58% Al
Optical burning rate (avg)	196	1269	1189	1024	802
Optical mass burning rate (avg)	129	740	585	487	350

B. Pressed Pellet Burns

The goal of this experiment was to determine the dependence of the burning rate on pressure. As described by Koch [21], the burning-rate pressure dependence of pyrotechnics can often be described by fitting a power-law curve to the data; specifically,

$$r_b = a \cdot P^n \tag{3}$$

where r_b is the burning rate, a is a coefficient that could depend on temperature, and n is the pressure exponent. This pressure-dependence correlation is also commonly used for propellant burning rates. Data from the AlTV experiments did not correlate well to the power-law model, and so a second-order polynomial fit was employed as well.

As stated before, high-speed imaging was recorded in order to determine the burning rates of the materials. Figure 10a shows a typical recorded image. A flat laminar flame front indicates uniform pellet composition, and it can also be seen that the inhibitor prevents the reaction from propagating down the edges of the pellet. The position of the flame front typically propagates at a reasonably constant rate. Also shown in Fig. 10b are representative data from the imaging that are used to calculate the burning rate. As expected, the burning rate increases as the pressure is increased, due to the increased collision frequency in the gas phase and subsequent feedback to the condensed phase and reactions with particle surfaces.

The results from the pressure-dependence experiments for SiTV and AlTV pellets are summarized with the plots in Fig. 11. As with the tube-burn data, the mass burning rate is less dependent on pellet density so the effect of varying mixture ratio and pressure can be highlighted. AlTV showed higher burning rates than SiTV, and both SiTV and AlTV have higher burning rates than MTV. All of the SiTV mixtures tested in this experiment behaved in a similar manner, following the power-law fit described earlier. The fact that the pressure exponents of the SiTV composites are near unity indicates that overall second-order gas-phase reactions are prevalent in the combustion, which is similar to many energetic materials.

Although not obvious from the plot, the AlTV data in Fig. 11b do not fit the power-law model as well as the SiTV data. This trend was seen in each AlTV mixture ratio tested and is indicative of a non-constant-pressure exponent, similar to that seen by Kubota and Serizawa [19] for MTV. One explanation for this result could be related to the flame standoff distance and flame coupling. This concept can be understood by studying Fig. 12. For decreasing pressures, the flame standoff distance of a burning material will increase. This will continue until the combustion becomes unstable, or until the gas-phase reaction, if still present, does not contribute to the propagation of the reaction and the burning rate. At these lower pressures (or Damköhler number Da), which vary for different materials, the pressure exponent will be close to zero (pressure-independent), because the pressure will not affect the burning rate of a condensed-phase-controlled reaction strongly. As pressure is increased, the flame will be closer to the surface and gas-phase reactions begin to influence the burning rate. The intermediate region with nearly constant slope is where many energetic materials deflagrate. The high-pressure regime consists of a surface flame for which burning rate is also independent of pressure, i.e., higher pressures do not continue to increase feedback to the surface.

The transitions between these three regions are predicted by some burning-rate models, such as the Ward–Son–Brewster (WSB) model

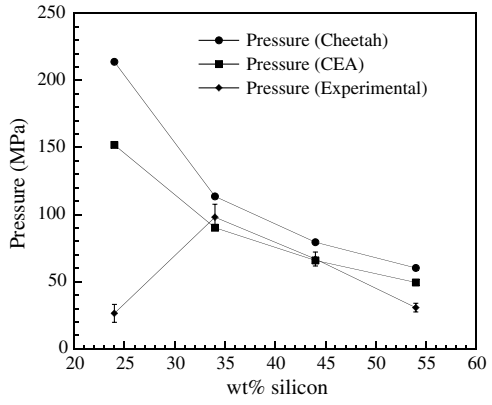

Fig. 9 Predicted and experimental pressures for SiTV tube-burn experiments.

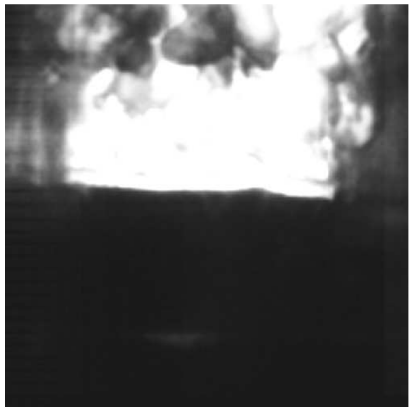

a) Here is an image from a pellet burn of SiTV with 24 wt% Si at 4.4 MPa

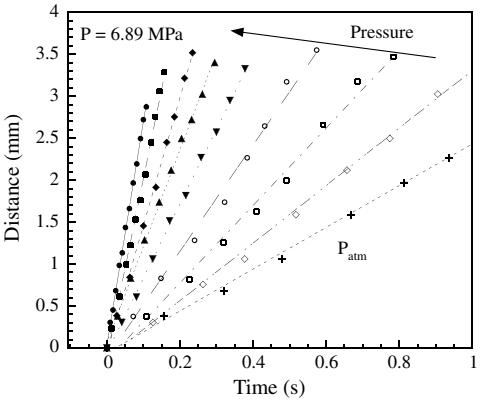

b) These are distance vs. time plots for SiTV, 24 wt% Si pressed pellets at various pressures for SiTV

Fig. 10 Typical pellet burn data.

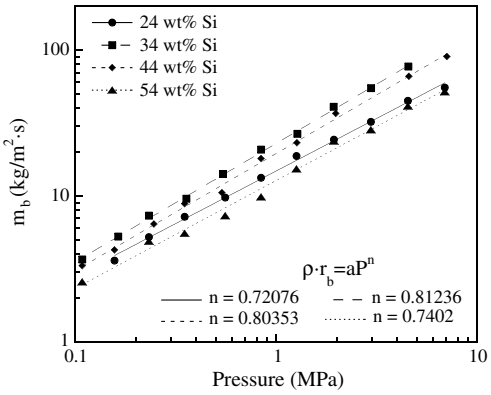

a) Mass burning rate as a function of pressure for SiTV pressed pellets

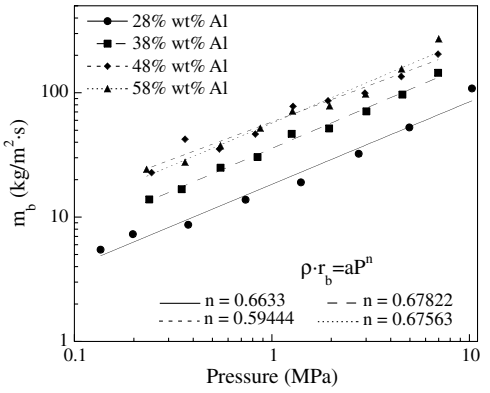

b) Mass burning rate as a function of pressure for AlTV pressed pellets

Fig. 11 SiTV and AlTV pellet burn data; maximum error is estimated to be ∼ ± 0.35 cm/s.

[31], to have a smooth transition from one condition to the other. Models assuming a high activation energy can also be formed for the three regions [32], but sharp transitions occur between regions, in contrast with the WSB model. If a material is tested in either of these transitional regions, one would expect to see a nonconstant-pressure exponent as the flame coupling varies. In particular, if a material is tested in the lower-pressure transition region, one would expect to see an increasing pressure exponent as gas-phase reactions begin to exert a greater influence. This behavior is less likely to be seen in materials in which most of the heat release is in the gas phase, such as typical propellants. In this case, when the pressure is low (sometimes just atmospheric pressure), deflagration becomes unstable, due to the decreased feedback from the gas phase, which is exacerbated by the small amount of heat release from the condensed phase. A transition would not be expected, but rather a lower-pressure deflagration limit beyond which combustion is either unsteady or not sustainable.

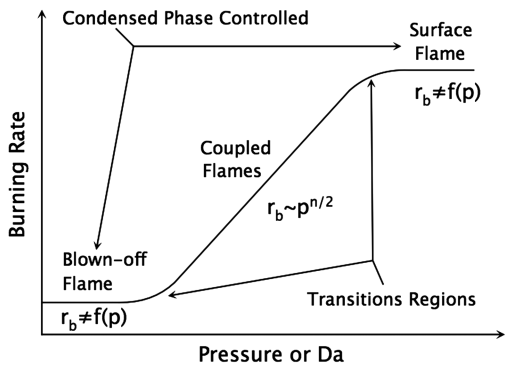

Fig. 12 Schematic of flame coupling as a function of pressure.

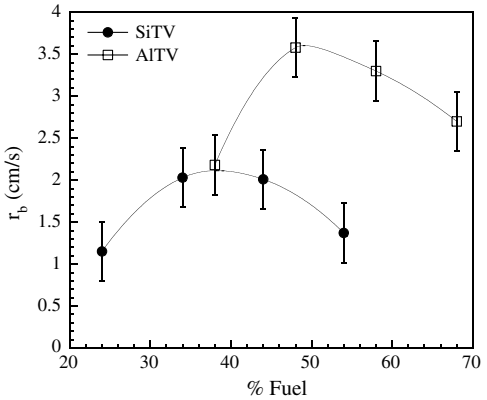

Fig. 13 Burning rates for SiTV and AlTV at 1.9 MPa.

One major difference between SiTV and AlTV is that as the fuel content in SiTV increases, the burning rate reaches a maximum value near 34 wt% Si, after which adding more fuel causes the burning rate to decrease (see Fig. 13). This is in contrast to MTV, in which the burning rate continued to increase with increasing fuel weight fraction, as reported by Kubota and Serizawa [19]. The peak for SiTV pellets also occurs in the same range as the maximum burning-rate peak for the loose-powder tube burns. The maximum burning-rate peak for AlTV pellets occurs at a much more fuel-rich mixture ratio than the loose-powder tube burns (58% vs 28%). Following the thermal theory of Mallard and Le Chatelier, as summarized by Kuo [33], one finds that for a premixed laminar flame, the burning rate should be proportional to $\sqrt{\alpha_g \cdot \Omega_g}$, where Ω_g is the gas-phase reaction rate. If the burning pellet is assumed to be gas-phase-controlled, this theory may provide insight to the combustion characteristics. If the thermal diffusivity varies enough to overcome a decreasing reaction rate at off-stoichiometric ratios, then the burning rate should still increase. When a similar analysis is done for a condensed-phase-controlled reaction, we find that the burning rate should be proportional to $\sqrt{\alpha_c \cdot \Omega_c}$, where Ω_c is the condensed-phase reaction rate. We find that the mass-averaged condensed-phase thermal diffusivities for SiTV and AlTV composites do not vary by a large enough amount to explain the difference in the peak burning-rate mixture ratio if a condensed-phase-controlled reaction is assumed for both AlTV and SiTV. This may be an indication of the presence and/or absence of condensed-phase-controlled reactions in SiTV and AlTV, resulting in dissimilar combustion behavior. As will be discussed in the following section, the likely scenario is that SiTV combustion is primarily gas-phase-controlled, whereas AlTV may be transitional, such that both gas phase and condensed phase play important roles, as discussed above.

One result reported by Kuwahara et al. [20] was that at very-fuel-rich conditions the burning-rate pressure dependence essentially disappears ($n = 0.06$) for MTV. One plausible explanation for this behavior is again linked to the condensed-phase reactions and transition between condensed/gas-phase-controlled burning. DSC and TGA results have been reported for both Al/PTFE and MTV that suggest a low-temperature preignition reaction or condensed-phase reaction occurs before the global (highest heat release) reaction proceeds [14,21]. This condensed-phase reaction is fairly exothermic and may have the potential to affect combustion behavior more than previously thought. At very-fuel-rich mixture ratios, this condensed-phase reaction may consume enough oxidizer to preclude the existence of a gas-phase reaction. This situation would result in a burning rate that was not affected by pressure, similar to Kuwahara et al.'s [20] results. In light of the previous discussion of nonconstant-pressure exponent, it is important to note that Huczko et al. [12] did not see a preignition reaction for Si/PTFE. Therefore, very-fuel-rich SiTV composites are not expected to be pressure-independent, but would instead reach a point at which the reaction would cease to be sustainable. Likewise at low pressures, it is expected that SiTV composites will behave more like typical propellants and reach a low-pressure deflagration limit.

V. Conclusions

Equilibrium calculations for SiTV and AlTV were performed to predict maximum temperature mixture ratios and products produced. It was found that the predicted maximum equilibrium temperature was higher for SiTV than AlTV. These maximum predicted temperatures occurred at 24 wt% Si and 28 wt% Al. Loose-powder burning rates were obtained for Si and Al fuels using PTFE as the oxidizer and FC 2175 as the binder. It was found that SiTV burning rates optimize at a fuel-rich mixture ratio, similar to other nano-energetic composite materials, particularly nanoscale Al thermites. AlTV optimized at roughly the stoichiometric mixture ratio for loose powders. Two separate initial propagation rates were found for AlTV, depending on the ignition mode used. One situation had a fast burning rate and high pressures and pressure slopes from start to finish, and the other started with slow burning rates and low pressures and pressure slopes, but then transitioned to the same fast burning rate. Peak AlTV pressures reached higher than 103 MPa. A peak pressure of 105 MPa for SiTV tube burns occurred at 34 wt% Si. Peak burning rates of $\sim$1269 m/s were measured for AlTV, and the peak average burning rate measured for SiTV was $\sim$1010 m/s at 34 wt% Si. Constant-volume equilibrium calculations were also performed. It was found that as long as propagation rates are fast enough, a constant-volume assumption is valid and experimental results match the calculations. If propagation rates are slow, the pressure dissipates and the combustion cannot be assumed to occur in a constant volume.

Pressed-pellet burning rates were also obtained at various pressures. Burning rates for SiTV and AlTV are generally faster than those for MTV, with AlTV being the fastest. SiTV composite burning rates showed a typical power-law dependence on pressure; however, the AlTV composite power-law dependence showed a nonconstant-pressure exponent. The nonconstant-pressure exponent of AlTV may be explained by flame coupling. If AlTV combustion occurs in a transitional region between a blown-off flame and a coupled flame, a nonconstant-pressure exponent would be expected. Burning rates of SiTV optimized at 34 wt% Si and did not continue to increase with increased wt% fuel, as others have seen for MTV. AlTV composites did increase with increased fuel content well past stoichiometric and optimized at 58 wt% Al. AlTV pellet burning rates decreased at 68 wt % Al. This difference is likely due to the presence of condensed-phase reactions in AlTV. Also in contrast to MTV, the SiTV pressure dependence remained essentially constant over the mixture ratios investigated. AlTV and SiTV did not show pressure-independent burning rates at mixture ratios tested; however, it is expected that AlTV will show this behavior due to the presence of condensed-phase reactions.

AlTV and SiTV may find pyrotechnic applications in various capacities. The hot corrosive combustion products as well as possible radiation make SiTV a good candidate for agent-defeat applications. Also, if either of the composites have spectral emission properties different from MTV, they may be used as replacements for MTV in flare applications.

Acknowledgments

The authors wish to acknowledge the funding of the Defense Threat Reduction Agency (DTRA), Counter-Weapons of Mass Destruction basic research program, grant number HDTRA1-08-1-0006. The support of Suhithi Peiris and Bill Wilson at DTRA are particularly noted. Also the staff of Los Alamos National Laboratories is acknowledged for their help in supporting this work. Finally, the technical staff at Zucrow Laboratory at Purdue University is acknowledged, including Rob and Ron McGuire, without whose help this work could not be accomplished.

References

[1] Koch, E.-C., and Clément, D., "Special Materials in Pyrotechnics: VI. Silicon—An Old Fuel with New Perspectives," *Propellants, Explosives, Pyrotechnics*, Vol. 32, No. 3, 2007, pp. 205–212. doi:10.1002/prep.200700021

[2] Al-Kazraji, S. S., and Rees, G. J., "The Fast Pyrotechnic Reaction of Silicon and Red Lead: Heats of Reaction and Rates of Burning," *Fuel*, Vol. 58, Feb. 1979, pp. 139–143. doi:10.1016/0016-2361(79)90238-2

[3] Rugunanan, R. A., and Brown, M. E., "Combustion of Binary and Ternary Silicon/Oxidant Pyrotechnic Systems, Part I: Binary Systems with Fe_2O_3 and SnO_2 as Oxidants," *Combustion Science and Technology*, Vol. 95, No. 1, 1994, pp. 61–83. doi:10.1080/00102209408935327

[4] Rugunanan, R. A., and Brown, M. E., "Combustion of Binary and Ternary Silicon/Oxidant Pyrotechnic Systems, Part II: Binary Systems with Sb_2O_3 and KNO_3 as Oxidants," *Combustion Science and Technology*, Vol. 95, No. 1, 1994, pp. 85–99. doi:10.1080/00102209408935328

[5] McCord, P., lin Tau, S., and Bard, A. J., "Chemiluminescence of Anodized and Etched Silicon: Evidence for a Luminescent Siloxene-Like Layer on Porous Silicon," *Science*, Vol. 257, No. 5066, 1992, pp. 68–69. doi:10.1126/science.257.5066.68

[6] Fan, G. J., Song, X. P., Quan, M. X., and Hu, Z. Q., "Explosive Reaction During the Mechanical Alloying of the Si/PbO System," *Scripta Materialia*, Vol. 35, No. 9, 1996, pp. 1065–1069. doi:10.1016/1359-6462(96)00267-9

[7] Kovalev, D., Timoshenko, V. Y., Kunzner, N., Gross, E., and Koch, F., "Strong Explosive Interaction of Hydrogenated Porous Silicon with Oxygen at Cryogenic Temperatures," *Physical Review Letters*, Vol. 87, No. 6, 2001, p. 068301. doi:10.1103/PhysRevLett.87.068301

[8] Moore, K., Pantoya, M. L., and Son, S. F., "Combustion Behaviors Resulting from Bimodal Aluminum Size Distributions in Thermites," *Journal of Propulsion and Power*, Vol. 23, No. 1, 2007, pp. 181–185. doi:10.2514/1.20754

[9] Mikulec, F. V., Kirtland, J. D., and Sailor, M. J., "Explosive Nanocrystalline Porous Silicon and Its Use in Atomic Emission Spectroscopy," *Advanced Materials*, Vol. 14, No. 1, 2002, pp. 38–41. doi:10.1002/1521-4095(20020104)14:1<38::AID-ADMA38>3.0.CO;2-Z

[10] Clément, D., Diener, J., Gross, E., Künzner, N., Timoshenko, V. Y., and Kovalev, D., "Highly Explosive Nanosilicon-Based Composite Materials," *Physica Status Solidi*, Vol. 202, No. 8, 2005, pp. 1357–1364. doi:10.1002/pssa.200461102

[11] Ksiazczak, A., Boniuk, H., and Cudziłło, S., "Thermal Decomposition of PTFE in the Presence of Silicon, Calcium Silicide, Ferrosilicon and Iron," *Thermal Analysis and Calorimetry*, Vol. 74, No. 2, 2003, pp. 569–574. doi:10.1023/B:JTAN.0000005195.46390.48

[12] Huczko, A., Lange, H., Chojecki, G., Cudziłło, S. C., Zhu, Y. Q., Walton, D. R. M., et al., "Combustion Synthesis of Nanostructures," *Structural and Electronic Properties of Molecular Nanostructures*, Vol. 633, American Inst. of Physics, Melville, NY, 2002, pp. 165–169.

[13] Bockmon, B., Pantoya, M., Son, S., Asay, B., and Mang, J., "Combustion Velocities and Propagation Mechanisms of Metastable Interstitial Composites," *Journal of Applied Physics*, Vol. 98, No. 6, 2005, Paper 064903. doi:10.1063/1.2058175

[14] Osborne, D. T., and Pantoya, M. L., "Effect of Al Particle Size on the Thermal Degradation of Al/Teflon Mixtures," *Combustion Science and Technology*, Vol. 179, No. 8, 2007, pp. 1467–1480. doi:10.1080/00102200601182333

[15] Zamkov, M. A., Conner, R. W., and Dlott, D. D., "Ultrafast Chemistry of Nanoenergetic Materials Studied by Time-Resolved Infrared Spectroscopy: Aluminum Nanoparticles in Teflon," *Journal of Physical Chemistry C*, Vol. 111, No. 28, 2007, pp. 10278–10284. doi:10.1021/jp072662h

[16] Dolgoborodov, A. Y., Makhov, M. N., Kolbanev, I. V., Streletskii, A. N., and Fortov, V. E., "Detonation in an Aluminum-Teflon Mixture," *JETP Letters*, Vol. 81, No. 7, 2005, pp. 311–314. doi:10.1134/1.1944069

[17] Watson, K. W., Pantoya, M. L., and Levitas, V. I., "Fast Reactions with Nano- and Micrometer Aluminum: A Study on Oxidation Versus Fluorination," *Combustion and Flame*, Vol. 155, No. 4, 2008, pp. 619–634. doi:10.1016/j.combustflame.2008.06.003

[18] Koch, E.-C., "Metal-Fluorocarbon-Pyrolants III: Development and Application of Magnesium/ Teflon/Viton (MTV)," *Propellants, Explosives, Pyrotechnics*, Vol. 27, No. 5, 2002, pp. 262–266. doi:10.1002/1521-4087(200211)27:5<262::AID-PREP262>3.0.CO;2-8

[19] Kubota, N., and Serizawa, C., "Combustion of Magnesium/ Polytetrafluoroethylene," *Journal of Propulsion and Power*, Vol. 3, No. 4, 1987, pp. 303–307.

doi:10.2514/3.22990
[20] Kuwahara, T., Matsuo, S., and Shinozaki, N., "Combustion and Sensitivity Characteristics of Mg/TF Pyrolants," *Propellants, Explosives, Pyrotechnics*, Vol. 22, No. 4, 1997, pp. 198–202. doi:10.1002/prep.19970220403
[21] Koch, E.-C., "Metal-Fluorocarbon-Pyrolants IV: Thermochemical and Combustion Behaviour of Magnesium/Teflon/Viton (MTV)," *Propellants, Explosives, Pyrotechnics*, Vol. 27, No. 6, 2002, pp. 340–351. doi:10.1002/prep.200290004
[22] Fried, L. E., Bastea, S., Glaesemann, K. R., Howard, W. M., Souers, P. C., and Vitell, P. A., *Cheetah 4.0 User's Manual*, Lawrence Livermore National Lab., Livermore, CA, 2004.
[23] "AIAA/ASME/SAE/ASEE, Combustion and Characterization of Nanoscale Aluminum and Ice Propellants," 44th AIAA/ASME/SAE/ASEE Joint Propulsion Conference & Exhibit, AIAA Paper 2008-5040, July 2008.
[24] Lide, D. R., *The Handbook of Chemistry and Physics*, CRC Press, Boca Raton, FL, and Taylor and Francis, London, 89th ed., 2008.
[25] Waterman, N., and Ashby, M. F., *The Material Selector*, 2nd ed., Chapman and Hall, Boca Raton, FL, 1997.
[26] Glassman, I., *Combustion*, 3rd ed., Academic Press, New York, 1996.
[27] "Ignition Pellets, Fluorocarbon-Magnesium," U.S. Department of Defense, MIL-PRF-82736A, 1985.
[28] Malchi, J. Y., Yetter, R. A., Foley, T. J., and Son, S. F., "The Effect of Added Al_2O_3 on the Propagation Behavior of an Al/CuO Nanoscale Thermite," *Combustion Science and Technology*, Vol. 180, No. 7, 2008, pp. 1278–1294. doi:10.1080/00102200802049471
[29] Sanders, V. E., Asay, B. W., Foley, T. J., Tappan, B. C., Pacheco, A. N., and Son, S. F., "Reaction Propagation of Four Nanoscale Energetic Composites (Al/MoO_3, Al/WO_3, Al/CuO, and Bi_2O_3)," *Journal of Propulsion and Power*, Vol. 23, No. 4, 2007, pp. 707–714. doi:10.2514/1.26089
[30] McBride, B. J., and Gordon, S., "Computer Program for Calculation of Complex Chemical Equilibrium Compositions and Applications," NASA RP-1311, 1996.
[31] Ward, M. J., Son, S., and Brewster, M. Q., "Role of Gas- and Condensed-Phase Kinetics in Burning Rate Control of Energetic Solids," *Combustion Theory and Modelling*, Vol. 2, No. 3, 1998, pp. 293–312. doi:10.1088/1364-7830/2/3/005
[32] Buckmaster, J. D., and Ludford, G. S. S., *Theory of Laminar Flames*, Cambridge Univ. Press, New York, 1982.
[33] Kuo, K. K., *Principles of Combustion*, 1st ed., Wiley, New York, 1986, pp. 289–291, Chap. 5.

C. Segal
Associate Editor